MmWave V2X Cooperative Diversity Relay Channel with Feedback Delay and Link Blockage

Elyes Balti, *Student Member, IEEE*

***Abstract*—In this work, we present a framework analysis of a millimeter wave (mmWave) vehicular communications systems. Communications between vehicles take place through a cooperative relay which acts as an intermediary base station (BS). The relay is equipped with multiple transmit and receive antennas and it employs decode-and-forward (DF) to process the signal. Also, the relay applies maximal ratio combining (MRC), and maximal ratio transmission (MRT), respectively, to receive and forward the signal. As the vehicles' speeds are relative high, the channel experiences a fast fading and this time variation is modeled following the Jake's autocorrelation model. We also assume narrowband fading channel. Closed-form expressions of the reliability metrics such as the outage probability and the mean rate are derived. Capitalizing on these performances, we derive the high signal-to-noise-ratio (SNR) asymptotes to get full insights into the system gains such as the diversity and coding gains.**

***Index Terms*—Millimeter wave, vehicular communications, decode-and-forward relaying, cooperative diversity, diversity gain.**

I. Introduction

The increase demand for bandwidth has been growing over the last few decades, largely due to the increased number of subscribers and number of communication devices. However, to meet these goals and the need for high-speed wireless data rate are challenging due to the limited spectrum.

Millimeter wave (mmWave) communications which refer to the wide spectrum between 28 and 300 GHz become a promising solution to provide high Gbps of bandwidth to emerging 5G network [1], [2]. Such interesting technology has recently attracted enormous attentions both in academia and industry [3]. High definition (HD) video applications leverage from mmWave frequencies to transmit ultra HD video to HDTV wirelessly [4]. In addition, mmWave can also replace fiber optic transmission lines connecting the core network to the backhaul when the cable installation is restricted or expensive [5]. Since mmWave spectrum becomes available for use, industries invested and produced mmWave based commercial products such as IEEE 802.11ad wireless gigabit alliance (WiGig) technology. In fact, this product is dedicated to support wireless display interfaces requiring high resolution and gigabit rate [3], [4], [6]. Furthermore, mmWave frequencies support radar applications for motion sensors, automatic doors, and collision avoidance systems [4], [7]. Moreover, mmWave communications have low interference and high security against hacking and intrusion. In fact, mmWave link has narrow beam and short range where the area experiences less interference from neighbor radios. Also, mmWave system is immune since the propagation is restricted to a limited area which enhances the security [4]. In the same context, mmWave technology has tremendous applications in vehicular communications area. Specifically, self-driving vehicles require a great amount of information from nearby vehicles and road side units (RSU) to enhance the vehicle awareness and avoid the potential accidents. Certainly such application requires a high bandwidth and data rate to support the big data exchanged between the vehicles and RSUs [7], [8].

Although mmWave technology has tremendous advantages, it suffers from many drawbacks. Due to the small wavelength, mmWave has a short propagation range around 20 meters for low power applications [9]. Supporting longer ranges requires large antenna gains and transmit power. Also, since mmWave frequencies are sensitive to blockage, it requires line of sight (LOS) communication as regular objects such as trees, human being, and building completely block the signal [2]. Consequently, the range is reduced and the received signal is weak. Furthermore, due to the high frequencies, mmWave is susbtantially degraded by the path loss as it suffers from the atmospheric attenuations such as the moisture, fog, rain attenuations, and the oxygen absorption [10]. To compensate for the path loss, mmWave systems use high directional array antennas. Moreover, due to the large bandwidth, the received mmWave signal experiences high noise degradations at the receiver which substantially limits the received signal-to-noise ratio (SNR).

To enhance the quality of the received signal, relay based cooperative communication technique has been proposed not only to improve the capacity but also to improve the coverage and assist the received signal power [28]. Related works have proposed various relaying techniques to process the signal such as amplify-and-forward (AF) [29], [30] and decode-and-forward (DF) [30]. The AF consists of amplifying the received signal with a proper gain factor and then forwards it, while DF decodes and denoises the signal and then forwards it. Since mmWaves are susceptible to the high noise power, the AF is not relevant because in this case the relay also amplifies the noise which is incorporated in the received signal.

In this context, we propose a dual-hop vehicular system wherein the relay employs DF relaying mode. The source and the destination are both a transmit (TX) and receive (RX) vehicles while the relay behaves as an intermediary base station (BS). The rest of this paper is organized as follows: the system model is presented in Section II. The reliability metrics

Elyes Balti is with the Wireless Networking and Communications Group, Department of Electrical and Computer Engineering, The University of Texas at Austin, Austin, TX 78712 USA e-mail: ebalti@utexas.edu.

analysis are detailed in Section III, while the discussion of the numerical results is reported in Section IV. Concluding remarks are presented in Section V.

II. System Model

Fig. 1 provides an illustration of the relay network.

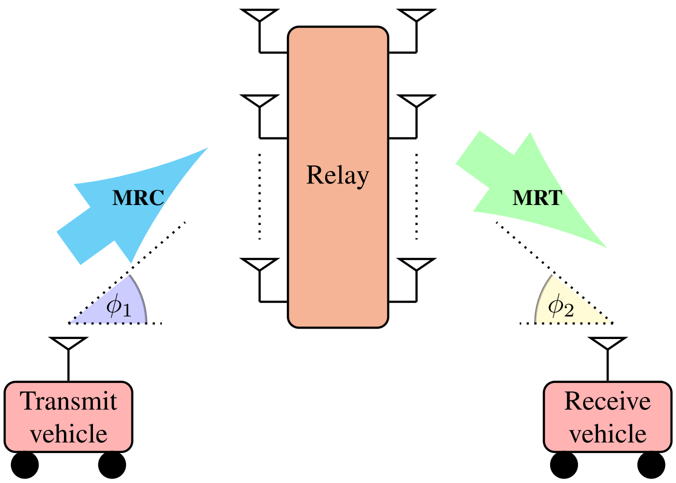

Fig. 1: Dual-hop millimeter wave vehicular relay channel.

The proposed system consists of two vehicles communicating through an intermediary relaying base station (BS). Each vehicle is equipped with a single antenna while the relay is equipped with multiple transmit (TX) and receive (RX) antennas, and employs DF protocol to process the received signal. We assume that the RX antennas elements are close enough and the distance between the relay and TX vehicle is long so that the angle of arrival and the time delay are the same for all the signals. The same assumption holds for the second hop, where the transmitted signals at the relay have the same angle of departure ϕ_2 and time delay to reach the receive vehicle. To estimate the channel state information (CSI), the relay sends periodic feedback to the vehicles. Since the feedback is slowly propagating and the channels are time-varying, the transmitted CSI will be the outdated version. The time correlation between the outdated and updated CSIs can be modeled using the Jake's autocorrelation model as follows [38, Eq. (8)]

$$\rho_i = [J_0(2\pi f_{d,i}\tau_{d,i})]^2, \tag{1}$$

where $J_0(\cdot)$ is the first kind of Bessel function with order zero, the index $i = 1,\ 2$ stands for the first and second hop. $f_{d,i} = \frac{f_c v_i \cos(\phi_i)}{c}$ is the doppler frequency, ϕ is the angle between vehicle displacement and the relay, f_c is the carrier frequency, v_i is the speed of the vehicle, c is the speed of light, and $\tau_{d,i}$ is the propagation delay.

Fig. 2 illustrates the time correlation with respect to the frequency and the vehicle speed. The maximum coherence time T_c corresponding to 28 GHz and a speed of 10 m/s, is 757.61 μs, while the minimum T_c corresponding to 73 GHz and a speed of 30 m/s is 193.73 μs. We observe that the correlation peaks decrease with the speed and the carrier frequency. As the vehicle speed increases mainly in highways and rural areas, the correlation decreases and inversely when the vehicle speed is lower, specifically in urban and sub-urban areas, the correlation improves. In fact, for higher speeds, the channel is rapidly varying and the estimation becomes worse. However, for lower speed, the TX and RX can relatively track the channel variations, and hence the estimation gets much better.

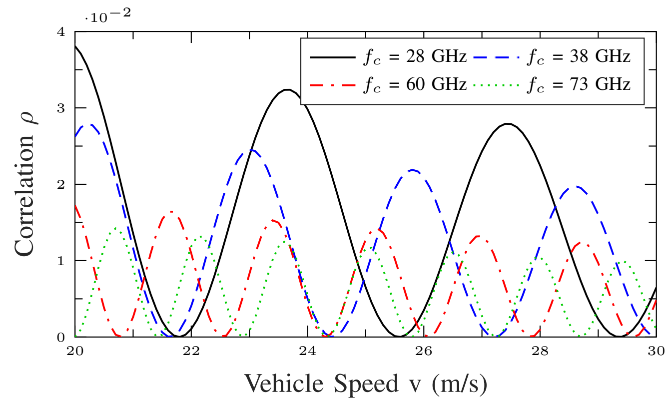

Fig. 2: Correlation dependence on the vehicle speed for different values of the carrier frequency. The symbol period T_s = 1 ms, τ_d = $2T_s$, and $\phi = \frac{\pi}{4}$.

The relation between the outdated $\hat{\gamma}_i$ and updated γ_i instantaneous SNRs of the hop i is expressed as follows [38, Eq. (7)]

$$\hat{\gamma}_i = \sqrt{\rho_i}\gamma_i + \sqrt{1-\rho_i}\omega_i \tag{2}$$

where ω_i is complex Gaussian distributed with zero-mean and having the same variance as γ_i.

A. Millimiter wave channel model of the hop i

Since the channels of the first and second hops are symmetric, and the relay transmit and receive strategies are also equivalent (MRC and MRT), we will focus the analysis on a single hop.

$$y_i = \sqrt{\frac{A_i P_i}{N_i}} \sum_{n=1}^{N_i} h_{n,i} s + \sum_{k=1}^{M_{r,i}} f_{k,i} d_{k,i} + n_i, \tag{3}$$

where A_i is the average power gain, P_i is the total transmitted power equally splitted among the N_i channels, s is the modulated symbol, $h_{n,i}$ is the n-th channel, $d_{k,i}$ is the modulated symbol of the k-th interferer with an average power $\mathbb{E}[|d_{k,i}|^2] = P_{k,i}$, $f_{k,i}$ is the fading coefficient of the k-th interferer, $M_{r,i}$ is the number of the interferers, and the noise n_i is a zero-mean additive white Gaussian noise (AWGN). The noise variance is given by

$$\sigma_i^2[\text{dBm}] = B + N_0 + N_f, \tag{4}$$

The path loss of the link i is given by [10]

$$PL_i[\text{dB}] = 20\log_{10}\left(\frac{4\pi f_c}{c}\right) + 10\sigma\log_{10}(L_i) - G_{t,i} - G_{r,i}, \tag{5}$$

where σ is the path loss exponent.

Table (I) summarizes the values of the system parameters used in the simulation.

TABLE I: System Parameters

Parameter	Symbol	Value
Transmit antenna gain	$G_{t,i}$	4 dB
Receive antenna gain	$G_{r,i}$	4 dB
Noise spectral density	N_0	-142 dBm/Hz
Noise figure	N_f	0 dB
Bandwidth	B	700 MHz
Speed of light	c	3 10^8 m/s
Link distance	L_i	50 m

B. Statistical analysis of the hop i

Given that the single input single output (SISO) channel fading is Nakagami-m distributed, the relative SNR follows the Gamma distribution. Hence the overall SNR, which is the sum of N_i Gamma identically distributed SNR per branch with scale m_i, is also a Gamma random variable with scale $N_i m_i$.

The joint probability density function (PDF) of the outdated and updated SNRs is given by [38, Eq. (14)]

$$f_{\hat{\gamma}_i,\gamma_i}(x,y) = \left(\frac{m_i}{\overline{\gamma}_i}\right)^{m_i+1} \frac{\left(\frac{xy}{\rho_i}\right)^{\frac{m_i-1}{2}}}{(1-\rho_i)\Gamma(m_i)} e^{-\left(\frac{x+y}{1-\rho_i}\right)\frac{m_i}{\overline{\gamma}_i}} \times I_{m_i-1}\left(\frac{2m_i\sqrt{\rho_i xy}}{(1-\rho_i)\overline{\gamma}_i}\right), \tag{6}$$

where $I_\nu(\cdot)$ is the ν-th order modified Bessel function of the first kind and $\overline{\gamma}_i$ is the average SNR. After some mathematical manipulations, the PDF of the outdated CSI is obtained by

$$f_{\hat{\gamma}_i}(x) = \left(\frac{N_i m_i}{\overline{\gamma}_i}\right)^{N_i m_i} \frac{x^{N_i m_i} - 1}{\Gamma(N_i m_i)} e^{-\frac{N_i m_i x}{(1-\rho_i)\overline{\gamma}_i}}, \tag{7}$$

Integrating (7) and using [39, Eq. (3.351.1)], the cumulative distribution function (CDF) is given by

$$F_{\hat{\gamma}_i}(x) = \frac{(1-\rho_i)^{N_i m_i}}{\Gamma(N_i m_i)} \gamma\left(N_i m_i,\ \frac{N_i m_i x}{(1-\rho_i)\overline{\gamma}_i}\right), \tag{8}$$

where $\gamma(\cdot,\cdot)$ is the incomplete lower gamma function. Since $N_i m_i$ is an integer, the CDF (8) can be reformulated as follows

$$F_{\hat{\gamma}_i}(x) = \left(1 - e^{-\frac{N_i m_i x}{(1-\rho_i)\overline{\gamma}_i}} \sum_{n=0}^{N_i m_i - 1} \frac{x^n}{n!}\left(\frac{N_i m_i}{(1-\rho_i)\overline{\gamma}_i}\right)^n\right) \times\ (1-\rho_i)^{N_i m_i}, \tag{9}$$

We assume that each interferer fading follows Nakagami-m with parameter $m_{r,i}$ and we neglect the impact of the time correlation on each channel. Repeating the same derivation steps, the PDF of the aggregate M_{r_i} interferers' SNR $\gamma_{r,i}$ is given by

$$f_{\gamma_{r,i}}(x) = \left(\frac{M_{r,i}m_{r,i}}{\overline{\gamma}_{r,i}}\right)^{M_{r,i}m_{r,i}} \frac{x^{M_{r,i}m_{r,i}-1}}{\Gamma(M_{r,i}m_{r,i})} e^{-\frac{M_{r,i}m_{r,i}x}{\overline{\gamma}_{r,i}}}, \tag{10}$$

where $\overline{\gamma}_{r,i}$ is the average SNR of the interferers.

The effective signal-to-interference-plus-noise-ratio (SINR) is expressed by

$$\gamma_{\text{eff},i} = \frac{\hat{\gamma}_i}{\gamma_{r,i}+1}, \tag{11}$$

Using [39, Eq. (3.351.3)], and after some mathematical manipulations, the CDF of the effective SINR is given by

$$\begin{aligned} F_{\gamma_{\text{eff},i}}(x) &= (1-\rho_i)^{N_i m_i} \Bigg[1 - \left(\frac{M_{r,i}m_{r,i}}{\overline{\gamma}_{r,i}}\right)^{m_{r,i}} \frac{1}{\Gamma(M_{r,i}m_{r,i})} \\ &\times \sum_{n=0}^{N_i m_i-1} \sum_{p=0}^{n} \frac{\binom{n}{p}}{n!} \left(\frac{N_i m_i}{(1-\rho_i)\overline{\gamma}_i}\right)^n \Gamma(M_{r,i}m_{r,i}+p) \\ &\times x^n \left(\frac{M_{r,i}m_{r,i}}{\overline{\gamma}_{r,i}} + \frac{N_i m_i x}{(1-\rho_i)\overline{\gamma}_i}\right)^{-(M_{r,i}m_{r,i}+p)} e^{-\frac{N_i m_i x}{(1-\rho_i)\overline{\gamma}_i}}\Bigg], \end{aligned} \tag{12}$$

Differentiating (12) and after some mathematical manipulations, the PDF of the effective SINR is given by

$$\begin{aligned} f_{\gamma_{\text{eff},i}}(x) &= \left(\frac{N_i m_i}{\overline{\gamma}_i}\right)^{N_i m_i} \left(\frac{M_{r,i}m_{r,i}}{\overline{\gamma}_{r,i}}\right)^{M_{r,i}m_{r,i}} \frac{x^{N_i m_i - 1}}{\Gamma(N_i m_i)} \\ &\times \frac{e^{-\frac{N_i m_i x}{(1-\rho_i)\overline{\gamma}_{r,i}}}}{\Gamma(M_{r,i}m_{r,i})} \sum_{p=0}^{m} \binom{m}{p} \Gamma(M_{r,i}m_{r,i}+p) \\ &\times \left(\frac{M_{r,i}m_{r,i}}{\overline{\gamma}_{r,i}} + \frac{N_i m_i x}{(1-\rho_i)\overline{\gamma}_i}\right)^{-(M_{r,i}m_{r,i}+p)}, \end{aligned} \tag{13}$$

Using the identity $\frac{\gamma(s,x)}{x^s} \backsim \frac{1}{s}$ as $x \to 0$, at high SNR, (8) can be expressed as

$$F_{\hat{\gamma}_i}(x) \backsim \frac{1}{(N_i m_i)!}\left(\frac{N_i m_i x}{\overline{\gamma}_i}\right)^{N_i m_i}, \tag{14}$$

After considering (11) and repeating the same derivation steps, the high SNR asymptote of the CDF of the effective SINR is given by

$$\begin{aligned} F_{\gamma_{\text{eff},i}}(x) &\backsim \frac{1}{\Gamma(M_{r,i}m_{r,i})(N_i m_i)!}\left(\frac{N_i m_i x}{\overline{\gamma}_i}\right)^{N_i m_i} \\ &\times \sum_{p=0}^{N_i m_i} \binom{N_i m_i}{p} \Gamma(M_{r,i}m_{r,i}+p) \left(\frac{\overline{\gamma}_{r,i}}{M_{r,i}m_{r,i}}\right)^p, \end{aligned} \tag{15}$$

From (15), the diversity gain per hop $G_{d,i}$ is

$$G_{d,i} = N_i m_i, \tag{16}$$

C. Symbol error probability of hop i

For M-QAM modulations, the average symbol error is expressed as

$$P_{e,i} = \alpha \mathbb{E}_{\gamma_{\text{eff},i}}\left[\mathcal{Q}(\sqrt{\beta\gamma})\right], \tag{17}$$

where $\mathcal{Q}(\cdot)$ is the Gaussian Q-function, and $\alpha,\ \beta$ stand for the modulation schemes. Using the integration by part, the symbol error can be reformulated as follows

$$P_{e,i} = \frac{\alpha\sqrt{\beta}}{2\sqrt{2\pi}} \int_0^\infty \frac{e^{-\frac{\beta\gamma}{2}}}{\sqrt{\gamma}} F_{\gamma_{\text{eff},i}}(\gamma)d\gamma, \tag{18}$$

Inserting (12) in (18) and after using [39, Eq. (7.813.1)], and [40, Eq. (07.43.03.0271.01)], the symbol error is given by

$$P_{e,i} = \frac{\alpha\sqrt{\beta}(1-\rho)^{N_i m_i}}{2\sqrt{2\pi}} \left(\Gamma(0.5)\sqrt{\frac{2}{\beta}} - \sum_{n=0}^{N_i m_i - 1} \sum_{p=0}^{n} \frac{\binom{n}{p}}{n!} \right.$$
$$\times \frac{\left(\frac{\overline{\gamma}_{r,i}}{m_{r,i}}\right)^p}{\Gamma(M_{r,i}m_{r,i})} \left(\frac{N_i m_i}{(1-\rho_i)\overline{\gamma}_i}\right)^n \left(\frac{\beta}{2} + \frac{N_i m_i}{(1-\rho_i\overline{\gamma}_i)}\right)^{-(n+\frac{1}{2})}$$
$$\left. \times G_{2,1}^{1,2}\left(\frac{N_i m_i \overline{\gamma}_{r,i}}{(1-\rho_i)M_{r,i}m_{r,i}\overline{\gamma}_i}\left(\frac{\beta}{2} + \frac{N_i m_i}{(1-\rho_i)\overline{\gamma}_i}\right) \middle| \begin{matrix}\kappa_1 \\ \kappa_2\end{matrix}\right)\right), \quad (19)$$

where $G_{p,q}^{m,n}(\cdot|-)$ is the Meijer-G function, $\kappa_1 = \left[\frac{1}{2} - n,\ 1 - M_{r,i}m_{r,i} - p\right]$, and $\kappa_2 = 0$.

At high SNR, the error probability can be expressed as

$$P_{e,i} \cong (G_{c,i}\overline{\gamma}_i)^{-G_{d,i}}, \quad (20)$$

where $G_{c,i}$ is the coding gain. After inserting (15) in (18), the high SNR error is derived as follows

$$P_{e,i} = \frac{\alpha\Gamma(N_i m_i + \frac{1}{2})}{2\sqrt{\pi}(N_i m_i)!}\left(\frac{2N_i m_i}{\beta\overline{\gamma}_i}\right)^{N_i m_i} \sum_{p=0}^{N_i m_i} \binom{N_i m_i}{p}$$
$$\times \frac{\Gamma(M_{r,i}m_{r,i} + p}{\Gamma(M_{r,i}m_{r,i})}) \left(\frac{\overline{\gamma}_{r,i}}{m_{r,i}}\right)^p, \quad (21)$$

After identifying (21) with (20), the coding gain is given by

$$G_{c,i} = \frac{\beta}{2N_i m_i}\left(\frac{2\Gamma(M_{r,i}m_{r,i})(N_i m_i)!\sqrt{\pi}}{\alpha\Gamma(N_i m_i + \frac{1}{2})}\right)^{\frac{1}{m}}$$
$$\times \left(\sum_{p=0}^{N_i m_i}\binom{N_i m_i}{p}\Gamma(M_{r,i}m_{r,i} + p)\left(\frac{\overline{\gamma}_{r,i}}{M_{r,i}m_{r,i}}\right)^p\right)^{\frac{1}{m}}, \quad (22)$$

D. Capacity of hop i

The average rate $\mathcal{C}_i$, expressed in (bps), is defined as the maximum error-free data rate transmitted by the system. Assuming Gaussian signaling, the mean rate can be written as follows

$$\mathcal{C}_i = B\mathbb{E}_{\gamma_{\text{eff},i}}\left[\log_2(1+\gamma)\right], \quad (23)$$

The derivation of the closed-form expression involves three main steps. The first one is to insert (13) in (23). Secondly, we convert each function of the integral into Fox-H function form. Finally, after applying the identity [41, Eq. (2.3)], the capacity is given by (24). Note that the function $H_{p1:q1,p2,q2:p3,q3}^{m1,n1:m2,n2:m3,n3}(-|-|-|\cdot,\cdot)$ is called the bivariate Fox-H function. An efficient MATLAB implementation of this function is given by [42, Appendix B].

E. Blockage model

MmWave communications are very sensitive to blockage. Consequently, it is important to consider this factor in the analysis to get consistent results. In this work, we adopt the exponential blockage model ($P_{\text{los}} = e^{-d/\delta}$), where P_{los} is the probability of line of sight (LOS). According to 3GPP, $\delta = 200$ m in suburban area [10].

III. Reliability Metrics Analysis

In this section, we provide the performance analysis of the proposed system, in particular, we consider the end-to-end outage probability, the probability of symbol error, and the ergodic capacity for the overall relay system. Basically, the statistical results derived in the previous section will be considered to get the reliability metrics and to quantify the performance losses and the system gains.

A. Outage probability analysis

The outage probability is defined as the probability that the overall SINR falls below a given threshold x. This threshold is a standard value designed to target a desirable quality of service.

$$\mathcal{C}_i = \frac{B(1-\rho_i)^{N_i m_i}}{\log(2)\Gamma(N_i m_i)\Gamma(M_{r,i}m_{r,i})}\sum_{p=0}^{N_i m_i}\binom{N_i m_i}{p}\left(\frac{\overline{\gamma}_{r,i}}{M_{r,i}m_{r,i}}\right)^p$$
$$\times H_{1,0:1,1:2,2}^{0,1:1,1:1,2}\left(\begin{matrix}(1-N_i m_i;1,1) \\ -\end{matrix}\middle|\begin{matrix}(1-M_{r,i}m_{r,i}-p,1) \\ (0,1)\end{matrix}\middle|\begin{matrix}(1,1),\ (1,1) \\ (1,1),\ (0,1)\end{matrix}\middle|\frac{\overline{\gamma}_{r,i}}{M_{r,i}m_{r,i}}, \frac{(1-\rho_i)\overline{\gamma}_i}{N_i m_i}\right), \quad (24)$$

Since LOS and NLOS propagations are assumed, the average CDF per hop is given by

$$F_{\gamma_{\text{eff},i}}(x) = P_{\text{los}}F_{\gamma_{\text{eff},i}}^{\text{los}}(x) + (1-P_{\text{los}})F_{\gamma_{\text{eff},i}}^{\text{nlos}}(x), \quad (25)$$

where $F_{\gamma_{\text{eff},i}}^{\text{los}}(\cdot)$ and $F_{\gamma_{\text{eff},i}}^{\text{nlos}}(\cdot)$ are the CDF of hop i evaluated respectively, for LOS and NLOS.

The overall SINR γ_e for the relay system employing DF protocol is given by

$$\gamma_e = \min\left(\gamma_{\text{eff},1},\ \gamma_{\text{eff},2}\right), \quad (26)$$

Consequently, the CDF of γ_e is given by

$$F_{\gamma_e}(x) = F_{\gamma_{\text{eff},1}}(x) + F_{\gamma_{\text{eff},2}}(x) - F_{\gamma_{\text{eff},1}}(x)F_{\gamma_{\text{eff},2}}(x), \quad (27)$$

Finally, the outage probability is obtained by

$$P_{\text{out}}(x) = \text{Prob}[\gamma_e < x] = F_{\gamma_e}(x), \quad (28)$$

B. Symbol error probability

Closed-form expression of the symbol error for the overall relay system is too long. Due to the space limitation, we will consider the following CDF approximation

$$F_{\gamma_e}(x) \cong F_{\gamma_{\text{eff},1}}(x) + F_{\gamma_{\text{eff},2}}(x), \tag{29}$$

Then, the overall symbol error can be obtained by

$$P_e \cong P_{e,1} + P_{e,2}, \tag{30}$$

C. Ergodic capacity

Since DF is assumed, the overall capacity of the relay channel can be expressed as follows

$$\mathcal{C} = \min\left(\mathcal{C}_1,\ \mathcal{C}_2\right), \tag{31}$$

D. System gains

The overall diversity gain G_d is given by

$$G_d = \min\left(G_{d,1},\ G_{d,2}\right), \tag{32}$$

while the overall coding gain G_c is obtained by

$$G_c = \begin{cases} G_{c,1} & G_{d,1} < G_{d,2} \\ \left(G_{c,1}^{-G_d} + G_{c,2}^{-G_d}\right)^{-\frac{1}{G_d}} & G_{d,1} = G_{d,2} \\ G_{c,2} & G_{d,1} > G_{d,2} \end{cases} \tag{33}$$

IV. Numerical Results

In this section, we present the analytical results of the reliability metrics following their discussion. The Nakagami-m parameters are 4 and 2, respectively, for LOS and NLOS propagations. For the interferers, the Nakagami-m parameter is equal to 1. The path loss exponents are 2 and 4, respectively, for LOS and NLOS.

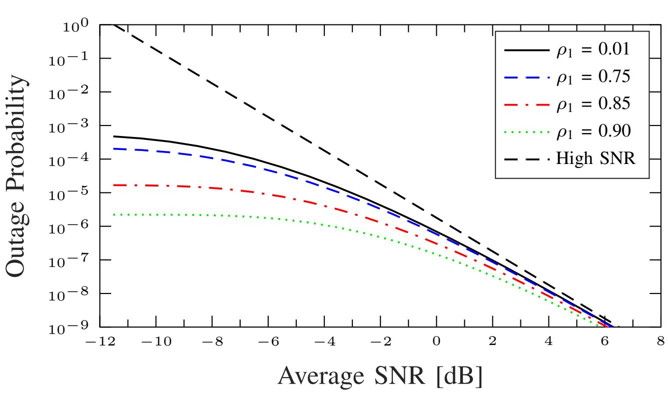

Fig. 3: Outage probability versus the average SNR for various time correlation values. The carrier frequency is 60 GHz and the link range is 50 m. The number of transmit and receive antennas are 5 and the time correlation for the second hop ρ_2 = 0.7. Two interferers are assumed with an average receive SNR of 0 dB and the outage threshold is - 50 dB.

Fig. 3 shows the dependence of the outage probability with respect to the time correlation of the first hop. The results show that the outage performance gets much worse when the channel estimation is bad, while the performance improves as the system becomes more or less able to track the channel variations and gets a better version of the estimated channel.

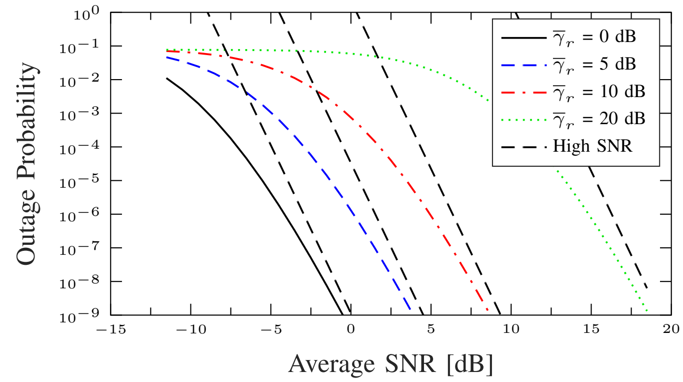

Fig. 4: Outage probability versus the average SNR for different receive SNR values of the interferers. The carrier frequency is 60 GHz and the link range is 50 m. The number of transmit and receive antennas are 5 and the time correlation is $\rho_1 = \rho_2$ = 0.1. The outage threshold is - 50 dB.

Fig. 4 illustrates the impacts of the power interferers on the outage performance. We observe that when the system is saturated by a large received power of the interferers, the outage deteriorates. Inversely, when the receiver becomes less susceptible to interferers (less power), the system performance gets much better.

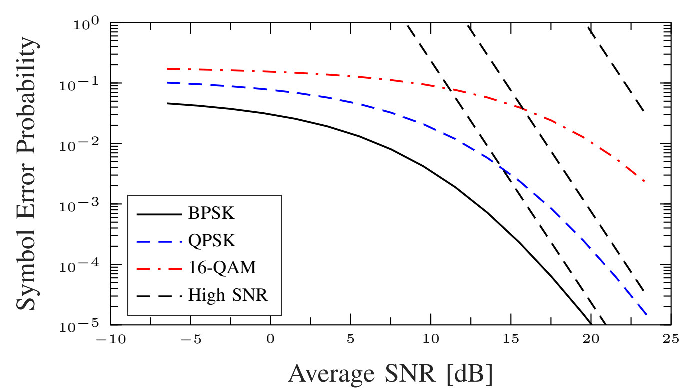

Fig. 5: Probability of symbol error versus the average SNR for different modulation schemes. The carrier frequency is 38 GHz and the link range is 50 m. The time correlation ais $\rho_1 = \rho_2$ = 0.5. We assume only LOS propagation in this scenario.

Fig. 5 shows the variations of the symbol error for various modulation schemes. This result is expected as BPSK modulation outperforms QPSK and 16-QAM. Also, this result is considered as a benchmarking tool to verify the accuracy of the symbol error derivation.

Fig. 6 shows the outage performance for various number of transmit and receive antennas. These results show how much diversity gain achieved by the system scaled by the number of antennas. As the number of antennas increase, the system becomes robust enough to combat the fading and improve the error performance. To achieve a given outage of 10^{-3}, the system setting for 10 antennas ahieves an array gain around 15 dB compared to the single antenna configuration.

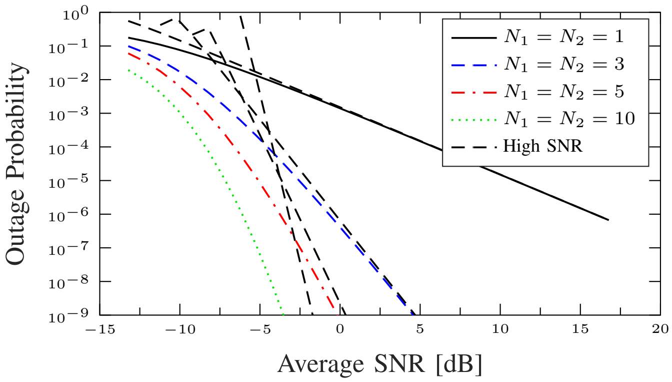

Fig. 6: Outage probability versus the average SNR for different number of transmit and receive antennas. The carrier frequency is 73 GHz and the link range is 50 m. The time correlation is $\rho_1 = \rho_2 = 0.1$, and the outage threshold is -50 dB.

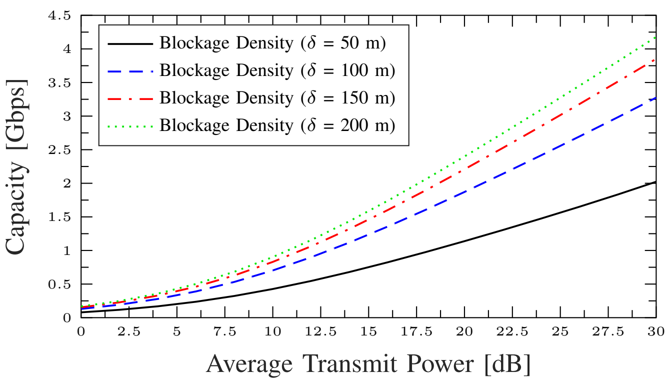

Fig. 7: Capacity versus the average SNR for different blockage densities. The carrier frequency is 28 GHz, the link range is 50 m, and the time correlation is $\rho_1 = \rho_2 = 10^{-3}$.

Fig. 7 illustrates the effects of the blockage density on the capacity. As the environment becomes more dense (lower δ) with physical objects, the capacity substantially decreases. This is explained by the fact that mmWaves are very sensitive to blockage. As the blockage becomes severe, the signal is completely attenuated. In addition, the system achieves high data rate of Gbps even though for severe blockage constraints.

V. Conclusion

In this work, we proposed a global framework analysis of a mmWave vehicular relay channel. We investigated the dependence of the reliability metrics on different parameters such as the number of antennas, the time correlation, the modulation, the power interferers, and the blockage density. We showed that the system becomes more resilient to fading by increasing the number of antennas and having a better channel estimation. Also, the performance improves when the receiver becomes less vulnerable to the interferers powers. Moreover, the capacity depends to a large extent on the blockage density, but, it is still in the order of Gbps even for severe blockage. As future directions, we intend to extend this work by considering wideband fading with transmit and receive beamforming designs to improve the channel capacity.

References

[1] Y. Niu, Y. Li, D. Jin, L. Su, and A. V. Vasilakos, "A survey of millimeter wave communications (mmWave) for 5G: opportunities and challenges," *Wireless Networks*, vol. 21, no. 8, pp. 2657–2676, Nov 2015.

[2] R. W. H. Jr., N. González Prelcic, S. Rangan, W. Roh, and A. M. Sayeed, "An Overview of Signal Processing Techniques for Millimeter Wave MIMO Systems," *CoRR*, vol. abs/1512.03007, 2015. [Online]. Available: http://arxiv.org/abs/1512.03007

[3] H. H. Meinel, "Millimeter wave applications and technology trends," *Annales Des Télécommunications*, vol. 47, no. 11, pp. 456–468, Nov 1992.

[4] "Applications of Millimeter Waves and Future." [Online]. Available: https://www.rfpage.com/applications-of-millimeter-waves-future/

[5] J. Beas, G. Castanon, I. Aldaya, A. Aragon-Zavala, and G. Campuzano, "Millimeter-Wave Frequency Radio over Fiber Systems: A Survey," *IEEE Communications Surveys Tutorials*, vol. 15, no. 4, pp. 1593–1619, Fourth 2013.

[6] K. Zeman, M. Stusek, J. Pokorny, P. Masek, J. Hosek, S. Andreev, P. Dvorak, and R. Josth, "Emerging 5G applications over mmWave: Hands-on assessment of WiGig radios," in *2017 40th International Conference on Telecommunications and Signal Processing (TSP)*, July 2017, pp. 86–90.

[7] J. Choi, V. Va, N. Gonzalez-Prelcic, R. Daniels, C. R. Bhat, and R. W. Heath, "Millimeter-Wave Vehicular Communication to Support Massive Automotive Sensing," *IEEE Communications Magazine*, vol. 54, no. 12, pp. 160–167, December 2016.

[8] V. Va, T. Shimizu, G. Bansal, and R. W. H. Jr., *Millimeter Wave Vehicular Communications: A Survey*. now, 2016.

[9] "The Role of Millimeter Waves in Ever-Expanding Wireless Applications." [Online]. Available: https://www.allaboutcircuits.com/news/the-role-of-millimeter-waves-in-ever-expanding-wireless-applications/

[10] T. S. Rappaport, Y. Xing, G. R. MacCartney, A. F. Molisch, E. Mellios, and J. Zhang, "Overview of Millimeter Wave Communications for Fifth-Generation (5G) Wireless Networks—With a Focus on Propagation Models," *IEEE Transactions on Antennas and Propagation*, vol. 65, no. 12, pp. 6213–6230, Dec 2017.

[11] S. Kwon and J. Widmer, "Relay selection for mmWave communications," in *2017 IEEE 28th Annual International Symposium on Personal, Indoor, and Mobile Radio Communications (PIMRC)*, Oct 2017, pp. 1–6.

[12] E. Balti and M. Guizani, "Mixed RF/FSO Cooperative Relaying Systems With Co-Channel Interference," *IEEE Transactions on Communications*, vol. 66, no. 9, pp. 4014–4027, Sept 2018.

[13] E. Balti, M. Guizani, B. Hamdaoui, and B. Khalfi, "Aggregate Hardware Impairments Over Mixed RF/FSO Relaying Systems With Outdated CSI," *IEEE Transactions on Communications*, vol. 66, no. 3, pp. 1110–1123, March 2018.

[14] N. S. Ferdinand, N. Rajatheva, and M. Latva-aho, "Effects of Feedback Delay in Partial Relay Selection Over Nakagami-m Fading Channels," *IEEE Transactions on Vehicular Technology*, vol. 61, no. 4, pp. 1620–1634, May 2012.

[15] D. Zwillinger, *Table of integrals, series, and products*, 7th ed. Academic Press, 2007.

[16] "The wolfram functions site." [Online]. Available: http://functions.wolfram.com

[17] P. K. Mittal and K. C. Gupta, "An integral involving generalized function of two variables," *Proceedings of the Indian Academy of Sciences - Section A*, vol. 75, no. 3, pp. 117–123, 1972.

[18] A. Soulimani, M. Benjillali, H. Chergui, and D. B. da Costa, "Performance Analysis of M-QAM Multihop Relaying over mmWave Weibull Fading Channels," *CoRR*, vol. abs/1610.08535, 2016.